Atmos. Chem. Phys. Discuss., doi:10.5194/acp-2016-289, 2016
Manuscript under review for journal Atmos. Chem. Phys.
Published: 18 April 2016

Atmospheric Chemistry and Physics Discussions

Complexities in the First Aerosol Indirect Effect over the Southern Great Plains

Sam Pennypacker[1] and Allison L. Steiner[2]

[1]University of Washington, Department of Atmospheric Sciences, Box 351640, Seattle, WA, 98195 USA
[2]University of Michigan, Department of Climate and Space Sciences and Engineering, Ann Arbor, MI, 48109, USA

Correspondence to: S. Pennypacker (spenny@uw.edu)

Abstract

The aerosol first indirect effect (FIE) is typically characterized by a reduction in cloud droplet size and an increase in cloud optical thickness in the presence of high concentrations of condensation nuclei. Past studies have derived observational evidence of the FIE in specific locations and conditions, yet critical uncertainties in the validity of this conceptual model as it applies to a range of cloud types and meteorological settings remain unaddressed. We utilize five years of surface aerosol measurements and Moderate Resolution Imaging Spectroradiometer (MODIS) observations of cloud properties to discern the FIE in springtime cloud statistics over the Southern Great Plains region of the United States. We extend this analysis to explore the role of three confounding factors: cloud phase, observational uncertainty and the role of regional meridional flow. While high aerosol days are dominated by smaller average droplet size in liquid clouds, the response of cloud optical thickness is variable and is dominantly a function of cloud water path. Ice clouds experience more variability in their response to high aerosol loading and satellite retrieval uncertainty thresholds. Finally, the direction of meridional flow does not play a large role in stratifying the cloud response to different aerosol loading. Overall, these observations show that much of the classical theory for liquid clouds is supported. Higher aerosol loadings are correlated with a reduction in effective radius and generally higher cloud optical thickness, and this relationship dominates over any driving influence from the low-level

Atmos. Chem. Phys. Discuss., doi:10.5194/acp-2016-289, 2016
Manuscript under review for journal Atmos. Chem. Phys.
Published: 18 April 2016

Atmospheric Chemistry and Physics Discussions

jet. However, for ice clouds we see a variable response that may be driven by aerosol composition and cold cloud microphysics. These observations provide further insight into the importance of considering deviations from the classic FIE in understanding regional variability in aerosol-cloud interactions in a continental setting.

1 Introduction

Under the classic paradigm, aerosols can both brighten clouds (Twomey, 1977) and lengthen cloud lifetime (Albrecht, 1989) by reducing droplet size and increasing droplet number. Along with the aerosol direct and semi-direct effects, understanding these so-called indirect effects is critical for studying Earth's energy budget and reducing uncertainty in global climate projections (Rosenfeld et al., 2014a). However, the effect of aerosols on clouds is sensitive to a variety of complicating factors, and a complete diagnosis of the physical system remains elusive (Stevens and Feingold, 2009). Critical uncertainties in the impact of aerosols on the lifetime of shallow clouds (Small et al., 2009) and the ability of aerosols to invigorate deep convection (Fan et al., 2013) remain. Competing effects of reduced precipitation formation efficiency and enhanced cloud-base evaporation make it difficult to fully determine aerosol-driven changes in liquid cloud water path (Han et al., 2002; Tao et al., 2012). Furthermore, aerosol effects on ice cloud properties (Lee and Penner, 2010; Storelvmo et al., 2011), the impact of measurement technique and uncertainty (Platnick et al., 2004) and the role of large-scale atmospheric conditions in modulating cloud microphysics (Jones et al., 2008; Muhlbauer et al., 2014) remain open questions. The first goal of this study is to observe which traditional FIE elements, including reduced droplet size and increased optical thickness, can be detected over the Southern Great Plains (SGP) by using liquid cloud field statistics as derived from satellite data. We then

Atmos. Chem. Phys. Discuss., doi:10.5194/acp-2016-289, 2016
Manuscript under review for journal Atmos. Chem. Phys.
Published: 18 April 2016

Atmospheric Chemistry and Physics Discussions

move beyond these variables to address whether cloud phase, measurement uncertainty and regional meteorology introduce substantial deviations from the standard FIE as determined from observations.

Observations of cloud microphysics under different aerosol conditions are abundant. Data on aerosol optical thickness (AOT), cloud effective radius (r_{eff}), cloud water path (CWP) and cloud optical thickness (COT) from a variety of satellite platforms have been used to develop correlative relationships between aerosol loading and cloud optical properties that show the first indirect effect at work (Chen et al., 2014; Jones et al., 2008; Kaufman and Koren, 2006; Koren et al., 2004, 2009; Rosenfeld, 2003). However, most of these studies reserve their analysis for warm clouds. Ice clouds play an important role in Earth's radiation budget (Liou, 2005), and it is likely their r_{eff}, CWP and COT respond to aerosols differently than liquid clouds (Gettelman et al., 2012). Both modeling (Storelvmo et al., 2011) and observational (Jiang et al., 2009) studies have suggested that an increase in available ice nucleation particles will decrease r_{eff} in ice clouds, in a similar fashion to their liquid counterparts. More work is needed to fully develop the relationship between aerosol composition, the balance of heterogeneous and homogeneous freezing and the net climatic effect (Gettelman et al., 2012; Zhou and Penner, 2014). It has been suggested that the heterogeneous activation of certain hydrophilic particles (e.g. mineral dust, organics) can reduce water concentrations and supersaturations necessary for homogenous activation (Chylek et al., 2006). This curtails the further formation of ice particles and limits the efficacy of a Twomey-like mechanism. Further observational statistics of ice cloud r_{eff}, CWP and COT are needed to clarify large-scale patterns of aerosol-ice cloud interactions.

Additionally, satellite retrievals are subject to some degree of uncertainty. For MODIS cloud products, both instrumental and retrieval algorithm error contributes to uncertainty (King

Atmos. Chem. Phys. Discuss., doi:10.5194/acp-2016-289, 2016
Manuscript under review for journal Atmos. Chem. Phys.
Published: 18 April 2016

Atmospheric Chemistry and Physics Discussions

et al., 1997; Platnick et al., 2004). The impact of this uncertainty depends on the product and the proposed application of the data. Assimilating MODIS observations into forecast products requires a low tolerance for uncertainty because of high model sensitivity to noisy initial conditions (Shi et al., 2011), and uncertainty thresholds for MODIS data products have developed over the instrument history (Chu, 2002; Remer et al., 2002; Tan et al., 2005). These thresholds motivate independent validation of the satellite retrievals and provide insight into the effect of product uncertainty on scientific conclusions. With this in mind, we can use thresholds to understand the role of retrieval uncertainty on observational understanding of the FIE.

Over the SGP, aerosol-cloud interactions occur against the backdrop of rapidly changing meteorology. The SGP region is known for its severe springtime convective weather, largely driven by synoptic-level disturbances moving with the jet stream (Doswell, 1980; Maddox, 1983). As spring transitions into summer, a major dynamical feature of the SGP region, the low-level jet (LLJ), evolves and brings warm, moist air off of the Gulf of Mexico (Weaver and Nigam, 2008) and defines the regional warm-season climate (Balling, 1985; Lee et al., 2008; Weaver et al., 2012). Large-scale dynamics set the stage for mesoscale activity by controlling factors critical to aerosol and cloud microphysics in varying degrees, including tropospheric stability (Chen et al., 2014), humidity (Altaratz et al., 2013) and vertical motion (Muhlbauer et al., 2014). The specific role of the largely meridional LLJ flow during the warm season (roughly May-September) in modulating aerosol-cloud interactions over this region has not been fully explored, however. Determining whether the LLJ influences r_{eff}, CWP and COT is a necessary prerequisite before attributing any bulk cloud response to changes in aerosol concentration.

In this manuscript, we use a unique combination of data to improve our understanding of the FIE in the SGP. By utilizing ground-based observations of aerosol concentrations and

Atmos. Chem. Phys. Discuss., doi:10.5194/acp-2016-289, 2016
Manuscript under review for journal Atmos. Chem. Phys.
Published: 18 April 2016

Atmospheric Chemistry and Physics Discussions

95 composition, and satellite-derived r_{eff}, LWP or IWP, we identify the cloud-aerosol interactions in
96 the SGP and develop an understanding of the role of meteorological conditions on the bulk cloud
97 response to changes in aerosol concentration.
98
99 **2 Methods**
100 **2.1 Aerosol Surface Concentrations and Event Identification**
101 To identify the role of aerosols in clouds, we use aerosol measurements from five
102 Interagency Monitoring of Protected Visual Environments (IMPROVE) sites in the Southern
103 Great Plains (Fig. 1; Table 1) to define climatological high and low aerosol events. All sites
104 report reconstructed $PM_{2.5}$ mass every three days, including speciated ammonium nitrate,
105 elemental and organic carbon, sulfate and soil (Malm et al., 1994). Springtime (April-May-June;
106 AMJ) averaged concentrations by composition are shown for each site in Fig. 2. By using
107 surface concentration data to determine an aerosol threshold, we assume that the IMPROVE
108 surface concentrations are indicative of concentrations aloft, and we discuss the validity of this
109 assumption in Sect. 4.1.
110 Evaluation of $PM_{2.5}$ data at each site over a decade (2003-2013) reveals an overall
111 downward trend in aerosol concentrations with a seasonal cycle that peaks in the summer
112 months. This overall decrease in aerosol is consistent with other studies over the continental US
113 showing a decrease in $PM_{2.5}$ concentrations over the past decade (Lamsal et al., 2015; Xing et al.,
114 2015). We focus our analysis on the convective season (April-May-June; AMJ), and use the
115 IMPROVE record to determine thresholds for minimum and maximum aerosol events. The first
116 half (2003-2008) of the observational record had noticeably higher concentrations than the latter
117 half (2008-2013), which could interfere with the determination of thresholds. We apply Eq. (1)

Atmos. Chem. Phys. Discuss., doi:10.5194/acp-2016-289, 2016
Manuscript under review for journal Atmos. Chem. Phys.
Published: 18 April 2016

Atmospheric Chemistry and Physics Discussions

118 to calculate the cumulative sum of deviations (S) and determine change points in data (Fealy and
119 Sweeney, 2005) (Figure 3)

$$S_i = \sum_{k=1}^{i} x_k - \bar{x}. \quad (1)$$

120 Positive slopes indicate that the individual aerosol concentration (x_k) for time k is above the
121 average aerosol concentration ($\bar{x}$), while negative slopes indicate the data is below average.
122 Extrema in the slope reveal change points in the data, and Fig. 3 illustrates that 2008 was a
123 change point in the time series of $PM_{2.5}$ data that is likely related to economic recession and
124 changes in air quality regulations (Russell et al., 2012). As a result we focus on the 2008-2013
125 data for statistical consistency. From 2008-2013, aerosol maximum events for each site are
126 determined by concentrations greater than one standard deviation above the 2008-2013 AMJ
127 average, and aerosol minimum events are marked by concentrations less than one standard
128 deviation below the same average. Aerosol maximum events have surface concentrations of
129 about 10 μg m^{-3} (individual sites ranging from 8.8-13.6 μg m^{-3}) and aerosol minimum events
130 have surface concentrations of about 2-4 μg m^{-3}. At each site, there are about 20-25 events of
131 each type during the five-year period, with the exception of the Tallgrass site, which has very
132 few days that meet the aerosol minimum threshold. Table 1 provides the details of each
133 IMPROVE site, including the number of identified minimum and maximum events and the
134 aerosol minimum and maximum thresholds used.
135

136 **2.2 MODIS Cloud Data**

137 Cloud data was retrieved from the Terra MODIS instrument (Platnick et al., 2015), with
138 retrieval algorithms discussed in King et al. (1997). In this study, we utilize cloud optical and
139 microphysical properties retrieved using the 0.645, 2.13 and 3.75 μm bands at 1 km resolution,

Atmos. Chem. Phys. Discuss., doi:10.5194/acp-2016-289, 2016
Manuscript under review for journal Atmos. Chem. Phys.
Published: 18 April 2016

Atmospheric Chemistry and Physics Discussions

including effective radius and cloud optical thickness (King et al., 1997). Cloud water path and phase is also derived at 1 km resolution using r_{eff} and CWP retrievals. Each retrieval value is tagged with a relative uncertainty value determined by contributions from both instrument and algorithm errors. Cloud top temperature is also derived at 5 km resolution.

On each aerosol maximum and minimum day, MODIS cloud properties are selected from 0.1° regions around each IMPROVE site, and both liquid and ice cloud field statistics are calculated. We compare all MODIS retrievals in the study window to data with less than 20% uncertainty in r_{eff} and COT, allowing an examination of the role of MODIS uncertainty on the observed FIE. Because CWP is derived from r_{eff} and COT, we did not constrain the data with CWP uncertainty. Given the three-day surface aerosol sampling time interval, it is more useful to compare distributions of cloud properties from a relatively large number of aerosol events over the five-year period rather than attempt to isolate effects from aerosols on individual events. We use a Kolmogorov-Smirnov analysis (Massey, 1951; Miller, 1956) to determine whether these distributions are statistically distinct. By defining F_1 and F_2 in Eq. (2) as the cumulative distribution functions for the aerosol minimum and maximum cloud property distributions, the D test statistic is compared to critical value tables to accept or reject the null hypothesis that the samples are statistically the same,

$$D = \max(|F_1(x) - F_2(x)|) \quad (2)$$

The null hypothesis that the minimum and maximum distributions are statistically the same is tested with a significance value (α) of 0.05.

Atmos. Chem. Phys. Discuss., doi:10.5194/acp-2016-289, 2016
Manuscript under review for journal Atmos. Chem. Phys.
Published: 18 April 2016

Atmospheric Chemistry and Physics Discussions

2.3 Meteorological Data and Microphysical Clustering

To determine the role of meteorology, we use daily average output from the North American Regional Reanalysis (NARR; Mesinger et al., 2006). The horizontal spatial resolution is 32 km in the horizontal with 29 vertical pressure levels. While much of the most important and potentially resolvable physics involved in cloud development and aerosol-cloud interactions is beyond the resolution of this reanalysis product, NARR accurately represents the larger scale atmospheric conditions such as wind speed and direction. In our analysis, we examine vertical profiles of temperature, specific humidity, and vertical, meridional and zonal winds in the SGP region.

To identify the potential role of meridional wind direction on cloud microphysics, we use k-means cluster analysis (Arthur and Vassilvitskii, 2007) on plots of average CTT vs. average r_{eff}. The clustering algorithm partitions data into a fixed number of clusters by minimizing the sum of squares between the data points and the cluster mean. Cloud top temperature-effective radius space allows us to visualize any potential interactions of the larger scale meteorology (e.g. meridional wind direction) with mean cloud properties and examine the continuum from liquid to ice clouds in a single framework. Any clusters based on the wind direction will help indicate the effect of NARR-determined meteorological conditions on aerosol-cloud interactions.

3 Results

3.1 Liquid Cloud Distributions

For each site, we evaluate the probability distribution of MODIS observations of r_{eff}, CWP and COT for aerosol minimum and maximum days with the 20% uncertainty filter at the five IMPROVE sites (Fig. 4). Kolmogorov-Smirnov tests indicate statistically distinct cloud

Atmos. Chem. Phys. Discuss., doi:10.5194/acp-2016-289, 2016
Manuscript under review for journal Atmos. Chem. Phys.
Published: 18 April 2016

Atmospheric Chemistry and Physics Discussions

properties between aerosol minimum and maximum days, both with and without (not shown) the uncertainty filter. One site (TALL) does not observe any liquid clouds for aerosol minimum events, so we discuss the four sites that have both aerosol minimum and maximum events. The MODIS domain-averaged filtered and unfiltered r_{eff} decreases at all sites where liquid clouds are detected on aerosol maximum days (Fig. 4a, Table 2), with greater site-to-site variation in the response of CWP and COT (Fig. 4b,c, Table 2). There is a decrease of average r_{eff} of 20-39% (filtered) and 10-19% (unfiltered) at the four sites with liquid clouds reported. At three of the four sites, the filtered average CWP decreases between 25-47% at three sites (CACR, UPBU and CEBL). A drop in average CWP generally corresponds to lower average COT on aerosol maximum days, with the unfiltered average CWP decreasing by 31-71% with a corresponding 15-62% decrease in COT at two of the four sites. However, at the CACR site, the decrease in CWP is accompanied by an increase in COT, which is inconsistent with the other sites. Additionally, a the WIMO site, the unfiltered average CWP increases 71% with a 118% increase in COT on aerosol maxima days. Therefore, while r_{eff} changes are as predicted for the FIE at all sites, the response in COT and CWP appear to be affected by other factors such as synoptic conditions as discussed in Section 3.3 below.

3.2 Ice Cloud Distributions

In contrast to the liquid phase retrievals, the sign of change in mean ice cloud effective radius is more sensitive to the uncertainty threshold, likely to due to the known uncertainties in ice cloud retrievals (Kahn et al., 2015; Platnick et al., 2004). When using an uncertainty threshold of 20%, three of the five sites (CACR, TALL and CEBL) show a 4-45% decrease in r_{eff} under higher aerosol loading and two sites (UPBU and WIMO) show a 6-31% increase in r_{eff}

Atmos. Chem. Phys. Discuss., doi:10.5194/acp-2016-289, 2016
Manuscript under review for journal Atmos. Chem. Phys.
Published: 18 April 2016

Atmospheric Chemistry and Physics Discussions

208 (Fig 5; Table 3). However, when all data is considered, the r_{eff} consistently decreases between
209 10-43% at all sites. KS tests determined that all of the distributions, both filtered and unfiltered
210 for uncertainty threshold, are statistically distinguishable. Compared to the liquid phase, there is
211 a consistent decrease in the average ice cloud water path to higher aerosol loading, with the
212 filtered average decreasing 17-63% at all sites under higher aerosol conditions and the unfiltered
213 data showing a 19-90% decrease at four of the sites (CACR, UPBU, WIMO, TALL). With the
214 filtered data, average COT drops between 12-62% on from aerosol minimum to maximum days
215 at four sites (UPBU, WIMO, TALL and CEBL) yet increases at one site (CACR; 66%). In
216 contrast, unfiltered COT increases between 1.8-50% at WIMO and CEBL but decreases between
217 79-85% at CACR, UPBU and TALL. Like the liquid phase, there are two sites (CACR, CEBL)
218 where an increase in COT is observed despite a decrease in CWP. Both are sites that are affected
219 by the uncertainty range, and we suspect that this may be due to retrieval error.
220
221 **3.3 Meteorological Conditions**
222 Because the CWP can play an important role in the COT response, this suggests that
223 synoptic conditions may also be affecting cloud properties in addition to aerosol loading. To
224 examine this question, we use the NARR to determine the effects of some synoptic indicators
225 such as zonal, meridional and vertical wind speeds (Figure 6). Generally, the differences in our
226 NARR-derived composite profiles between aerosol minimum and maximum days are most
227 pronounced at approximately 900 hPa and below. Above 900 hPa, the error bars (representing ±
228 one standard deviation) on the average profiles show greater overlap, suggesting little difference
229 in the conditions for these two event types. Profiles of specific humidity (not shown) suggest a
230 moister lower atmosphere when flow comes from the South, consistent with our expectations for

Atmos. Chem. Phys. Discuss., doi:10.5194/acp-2016-289, 2016
Manuscript under review for journal Atmos. Chem. Phys.
Published: 18 April 2016

231 the LLJ (Berg et al., 2015; Weaver and Nigam, 2008). However, above about 800 hPa, the
232 composite profiles are virtually indistinguishable between aerosol minimum and maximum days
233 at all sites. Two of the most pronounced features in the meteorological data are the average
234 meridional and vertical wind profiles at approximately 900 hPa. All sites exhibit strong southerly
235 flow on aerosol maximum days (59-91% of all days) consistent with the presence of the low
236 level jet in the region and peak windspeeds near the top of the planetary boundary layer (a
237 maximum of 7-10 m s^{-1} at approximately 900 hPa). In contrast, aerosol minimum days show
238 northerly flow with a weak jet (2-5 m s^{-1}) at 900 hPa at two sites, with three sites lacking any
239 distinct low-level jet, though 70-100% of the aerosol minimum days have at least weak northerly
240 flow (see Table 4). At the same altitude, aerosol maximum days show an area of downward
241 vertical motion of 0.05-0.2 m s^{-1} at all sites (Figure 6). This downward motion at around 900 hPa
242 is not evident for aerosol minimum days with the exception of the CEBL site, which shows a
243 slight (0.05 m s^{-1}) downward motion closer to 800 hPa.
244
245 **4 Discussion**
246 **4.1 Microphysical Regimes**
247 Satellite observations have suggested that convective clouds develop through distinct
248 microphysical regimes as described through the relationship between cloud top temperature
249 (CTT) and r_{eff}, with regimes defined as diffusion, collision-coalescence, warm rainout, mixed
250 phase and glaciation (Martins et al., 2011). It is important to note that not all five regimes are
251 necessarily present in each cloud system, depending on aerosol conditions (Rosenfeld and
252 Lensky, 1998). Other observations have supported Rosenfeld and Lensky's initial conclusions
253 (Suzuki et al., 2011) and this regime has been adapted and generalized in other work (Rosenfeld

Atmos. Chem. Phys. Discuss., doi:10.5194/acp-2016-289, 2016
Manuscript under review for journal Atmos. Chem. Phys.
Published: 18 April 2016

and Woodley, 2003; Rosenfeld et al., 2014b). Adopting this framework has two main benefits; we can compare average cloud top temperature and effective radius profiles between aerosol minimum and maximum days and examine whether the direction of the LLJ clusters the response of these clouds on these plots.

The observed r_{eff} vs. CTT for aerosol minimum (Fig. 7a) and aerosol maximum (Fig. 7b) during our time period of analysis across all sites is shown with approximate microphysical regimes as suggested by Martins et al. (2011). We see a similar relationship between the two variables as in prior studies, yet no clear distinction between our aerosol minimum and maximum events. We had hypothesized that the aerosol minimum and maximum events would separate as the theoretical moderately and heavily polluted microphysical regime curves (Rosenfeld et al., 2014b) reproduced in Fig. 7a,b, yet there is no clear distinction between the aerosol minimum and maximum events with respect to this framework. The lack of clear differences could be explained with several factors. The first is that the separation between aerosol minimum and maximum conditions as defined by the thresholds in Table 1 does not produce dramatic changes to the microphysical evolution of clouds. This indicates that the selection of minimum and maximum concentration thresholds may not follow the same definitions for clean, moderate pollution and heavy pollution, originally developed by Rosenfeld and Lensky (1998). They originally defined their pollution regimes based on a spectrum bounded by maritime clouds (clean) and clouds forming in the presence of smoke over land-based biomass burning (heavily polluted). Even on aerosol minimum days for the SGP sites, average total $PM_{2.5}$ concentration is 3.3 μg m^{-3}. Secondly, we assume that surface concentrations of aerosols are an indicator of CCN availability near clouds as they develop with time. Further work

Atmos. Chem. Phys. Discuss., doi:10.5194/acp-2016-289, 2016
Manuscript under review for journal Atmos. Chem. Phys.
Published: 18 April 2016

will be needed to test the strength of this assumption, especially for ice clouds whose formation is more detached from boundary layer aerosols.

Applying k-means analysis (for up to five statistically distinct clusters) does not reveal any clustering of mean cloud r_{eff} by meridional wind direction. This is despite the fact that aerosol maximum days are dominated by southerly flow, while aerosol minimum days are dominated by northerly flow. Given the lack of any clear influence of the meridional flow, it is likely that the aerosols are playing a role in bulk cloud field variability than the LLJ during this time of the year. This does not rule out the influence of other large-scale dynamical features as sources of variability in cloud microphysics (Muhlbauer et al., 2014), but it does implicate aerosols as a significant factor over the SGP. While we may be operating over a relatively narrow range of aerosol conditions from a global perspective, differences in cloud property distributions remain meaningful and statistically distinct by our local definition of aerosol minima and maxima.

4.2 Liquid and Ice Cloud Responses

Liquid clouds observed in this study exhibit the expected drop in effective radius under aerosol maximum conditions. One out of the four sites with the liquid phase registered has optically thicker clouds on these high aerosol events as well. The response of the COT is conditional on whether CWP increases or not, and we observe decreases in CWP at three out four sites with registered liquid clouds. The site (WIMO) that sees an increase in CWP does not have noteworthy differences in aerosol minimum and maximum concentration thresholds from the other sites (see Table 1). Modeling and observational studies of both shallow and deep clouds have suggested that liquid cloud water path should increase under high aerosol loading, and this

Atmos. Chem. Phys. Discuss., doi:10.5194/acp-2016-289, 2016
Manuscript under review for journal Atmos. Chem. Phys.
Published: 18 April 2016

299 is often attributed to a decrease in precipitation efficiency caused by smaller droplets within the
300 cloud (Lee et al., 2009; Tao et al., 2012). However, there are known mechanisms for decreasing
301 CWP under high aerosol conditions, including the influence of semi-direct effects (Koch and Del
302 Genio, 2010) and enhanced cloud-base evaporation of smaller droplets (Tao et al., 2012).

303 The response of the ice clouds to aerosol loading is inconsistent between the sites, with
304 only three out of five sites showing a decrease in effective radius under higher aerosol conditions
305 and considering only data with less than 20% uncertainty. Prior work suggests that ice cloud r_{eff}
306 does often exhibit similar responses to its liquid counterpart (Chylek et al., 2006; Jiang et al.,
307 2009; Storelvmo et al., 2011), yet our data show there may be more variability. This may be due
308 to the uncoupling between surface aerosols and cold cloud processes, as ice nuclei may be
309 transported from other locations aloft. At two of the five sites we observe an increase in effective
310 radius under high aerosol loading, raising the possibility of an “anti-Twomey" effect connected
311 to the dominant ice nucleation pathway and ice nucleation particle composition (Gettelman et al.,
312 2012; Panicker et al., 2010). At all sites and regardless of uncertainty threshold, we observe a
313 decrease in cloud water path in the ice phase on aerosol maximum events. At four out of fives
314 sites (UPBU, WIMO, TALL and CEBL) surface concentrations of combined soil and organics,
315 the particles typically associated with heterogeneous activation, tend to occur in higher
316 proportions than sulfate on aerosol maximum days, indicating it is possible that heterogeneous
317 freezing may be dominant. Heterogeneous freezing has been shown to decrease ice particle
318 concentration and increase ice particle size, leading to increased particle aggregation efficiency
319 and settling rate in climate models; this leads to reductions in ice cloud water path (Hendricks et
320 al., 2011). It is unclear whether the fraction of heterogeneous to homogeneous nucleation has a
321 definitive radiative effect in climate model simulations (Gettelman et al., 2012), though some

Atmos. Chem. Phys. Discuss., doi:10.5194/acp-2016-289, 2016
Manuscript under review for journal Atmos. Chem. Phys.
Published: 18 April 2016

322 ice-aerosol processes are clearly more sensitive to background activation processes (Zhou and
323 Penner, 2014). However, k-means clustering analysis does not reveal any significant
324 stratification of the the r_{eff} vs. CTT data in Fig. 7 if we use dominant chemical composition
325 instead of meridional wind direction as the basis for the clustering. This study is limited in its
326 ability to fully diagnose all the potential microphysical mechanisms at work, however, and more
327 investigation is needed before attribution can be made.

328 From the given MODIS retrievals, it is clear that the level of tolerance for data with high
329 uncertainty can alter both the magnitude and direction of changes in cloud properties over certain
330 sites. For example, average ice r_{eff} increases using data with less than 20% uncertainty but
331 decreases when considering the entire data set. Using observations to determine the feasibility of
332 a physical process (e.g. an anti-Twomey effect for ice clouds) requires careful consideration of
333 uncertainty thresholds, and it is clear more work is needed to better understand the impact of
334 measurement uncertainty on scientific conclusions.

335

336 *4.3 Effect of Meridional Flow*

337 The importance of the jet in the convective meteorology of this region is well-established
338 (Balling, 1985; Lee et al., 2008; Weaver and Nigam, 2008), and it is thus important to consider
339 any indirect roles the LLJ could be playing in setting the stage for observations of aerosol-cloud
340 interactions. Northward flow across this region is known to transport particulate matter over the
341 SGP, and it has been suggested the transport of biomass burning particles can impact tornado
342 formation (Saide et al., 2015). Furthermore, shear at the top of the planetary boundary layer
343 caused by low-level jets can induce downward vertical mixing and could allow for the build-up
344 of particulate matter and other pollutants in the lower atmosphere (Hu et al., 2013). This is

Atmos. Chem. Phys. Discuss., doi:10.5194/acp-2016-289, 2016
Manuscript under review for journal Atmos. Chem. Phys.
Published: 18 April 2016

consistent with the region of downward vertical motion we observe in the NARR wind speed profiles on aerosol maximum days (Fig. 6) at the same level as the highest LLJ shear. This interpretation requires some degree of confidence in the convective and turbulence parameterizations used in the development of NARR. The exact role of each of these mechanisms on the time scales we observe will require further work with back-trajectory analysis and new developments in LLJ dynamics (Klein et al., 2015).

5 Conclusions

We present MODIS observations of cloud effective radius, water path and optical thickness under surface aerosol minimum and maximum conditions over the Southern Great Plains region of the United States in the context of region meteorology derived from the North American Regional Reanalysis product. These data show a decrease in effective radius for liquid clouds with higher aerosol concentrations as expected from the traditional first indirect effect mechanism, with changes in cloud optical thickness tied to changes in cloud water path. The response of ice cloud properties is more variable, though measured surface aerosol composition coupled with observations of large reductions in ice cloud water path on aerosol maximum days suggests a heterogeneous freezing mechanism may be a driver of these inconsistencies. K-means cluster analysis does not reveal any direct relationship between meridional flow and mean cloud properties, indicating aerosols are likely playing an important role in springtime cloud variability. We also find that MODIS uncertainty threshold implementation has a strong potential to change scientific conclusions. Our results reemphasize the need for continuous improvement and testing of remote sensing products used for verifying models and drawing conclusions about aerosol-cloud-climate interactions. A great deal of progress has already been made in this regard,

particularly in the detection of cirrus clouds (Meyer and Platnick, 2010) and understanding the causes of MODIS retrieval failures (Cho et al., 2015). Determining causal links with relatively uncontrollable observational experiments is difficult, though this kind of work can reinforce and guide modeling efforts. We have shown that characterizing complexities in the traditional first indirect effect mechanism is possible through observations of aerosol concentrations and cloud properties combined with a reanalysis product. More work is needed to better understand the spatial and temporal variability of the impact of cloud phase, measurement uncertainty and regional meteorology on the traditional first indirect effect.

Data Availability

NCEP/NARR Reanalysis data provided by the NOAA/OAR/ESRL PSD, Boulder, Colorado, USA, from their Web site at http://www.esrl.noaa.gov/psd/. The IMPROVE Network is maintained by the National Park Service and the data can be accessed at http://vista.cira.colostate.edu/improve/Data/IMPROVE/improve_data.htm. Terra MODIS L2 cloud data (MOD06_L2) is available from NASA Goddard Space Flight Center at http://modis-atmos.gsfc.nasa.gov/MOD06_L2/acquiring.html.

Acknowledgements

Most of this work was done under the auspices of NSF Research Experience for Undergraduates (REU) award AGS 1358629.

References

Albrecht, B. A.: Aerosols, Cloud Microphysics, and Fractional Cloudiness, Science (80-.)., (4), 1227–1230, 1989.

Altaratz, O., Bar-Or, R. Z., Wollner, U. and Koren, I.: Relative humidity and its effect on aerosol optical depth in the vicinity of convective clouds, Environ. Res. Lett., 8(3), 034025, doi:10.1088/1748-9326/8/3/034025, 2013.

Arthur, D. and Vassilvitskii, S.: k-means++: The advantages of careful seeding, Proc. eighteenth Annu. ACM-SIAM Symp. Discret. algorithms, 8, 1027–1035, doi:10.1145/1283383.1283494, 2007.

Balling, R. C.: Warm Season Nocturnal Precipitation in the Great Plains of the United States, J. Clim. Appl. Meteorol., doi:10.1175/1520-0450(1985)024<1383:WSNPIT>2.0.CO;2, 1985.

Berg, L. K., Rihimaki, L. D., Qian, Y., Yan, H. and Huang, M.: The Low-Level Jet over the Southern Great Plains Determined from Observations and Reanalyses and Its Impact on Moisture

403 Transport, J. Clim., 28, 6682–6706, doi:10.1175/JCLI-D-14-00719.1, 2015.

404 Chen, Y.-C., Christensen, M. W., Stephens, G. L. and Seinfeld, J. H.: Satellite-based estimate of
405 global aerosol–cloud radiative forcing by marine warm clouds, Nat. Geosci., 7,
406 doi:10.1038/ngeo2214, 2014.

407 Cho, H., Zhang, Z., Meyer, K., Lebsock, M., Platnick, S., Ackerman, A. S., Girolamo, L. Di,
408 Laurent, C., Cornet, C., Riedi, J. and Holz, R. E.: Frequency and causes of failed MODIS cloud
409 property retrievals for liquid phase clouds over global oceans, J. Geophys. Res. Atmos., 120,
410 4132–4154, doi:10.1002/2015JD023161.Received, 2015.

411 Chu, D. a.: Validation of MODIS aerosol optical depth retrieval over land, Geophys. Res. Lett.,
412 29(12), 4–7, doi:10.1029/2001GL013205, 2002.

413 Chylek, P., Dubey, M. K., Lohmann, U., Ramanathan, V., Kaufman, Y. J., Lesins, G., Hudson,
414 J., Altmann, G. and Olsen, S.: Aerosol indirect effect over the Indian Ocean, Geophys. Res. Lett.,
415 33(6), 2–5, doi:10.1029/2005GL025397, 2006.

416 Doswell, C. A.: Synoptic-Scale Environments Associated with High Plains Severe
417 Thunderstorms, Bull. Am. Meteorol. Soc., 61(11), 1388–1400, doi:10.1175/1520-
418 0477(1980)061<1388:SSEAWH>2.0.CO;2, 1980.

419 Fan, J., Leung, L. R., Rosenfeld, D., Chen, Q., Li, Z., Zhang, J. and Yan, H.: Microphysical
420 effects determine macrophysical response for aerosol impacts on deep convective clouds., Proc.
421 Natl. Acad. Sci. U. S. A., 110(48), E4581–90, doi:10.1073/pnas.1316830110, 2013.

422 Fealy, R. and Sweeney, J.: Detection of a possible change point in atmospheric variability in the
423 North Atlantic and its effect on Scandinavian glacier mass balance, Int. J. Climatol., 25(14),
424 1819–1833, doi:10.1002/joc.1231, 2005.

425 Gettelman, A., Liu, X., Barahona, D., Lohmann, U. and Chen, C.: Climate impacts of ice
426 nucleation, J. Geophys. Res. Atmos., 117(20), 1–14, doi:10.1029/2012JD017950, 2012.

427 Han, Q., Rossow, W. B., Zeng, J. and Welch, R.: Three Different Behaviors of Liquid Water
428 Path of Water Clouds in Aerosol–Cloud Interactions, J. Atmos. Sci., 59(3), 726–735,
429 doi:10.1175/1520-0469(2002)059<0726:TDBOLW>2.0.CO;2, 2002.

430 Hendricks, J., Krcher, B. and Lohmann, U.: Effects of ice nuclei on cirrus clouds in a global
431 climate model, J. Geophys. Res. Atmos., 116(18), 1–24, doi:10.1029/2010JD015302, 2011.

432 Hu, X.-M., Klein, P. M., Xue, M., Zhang, F., Doughty, D. C., Forkel, R., Joseph, E. and Fuentes,
433 J. D.: Impact of the vertical mixing induced by low-level jets on boundary layer ozone
434 concentration, Atmos. Environ., 70(0), 123–130,
435 doi:http://dx.doi.org/10.1016/j.atmosenv.2012.12.046, 2013.

436 Jiang, J. H., Su, H., Massie, S. T., Colareo, P. R., Schoeberl, M. R. and Platnick, S.: Aerosol-CO
437 relationship and aerosol effect on ice cloud particle size: Analyses from Aura Microwave Limb
438 Sounder and Aqua Moderate Resolution Imaging spectroradiometer observations, J. Geophys.
439 Res. Atmos., 114(20), 1–8, doi:10.1029/2009JD012421, 2009.

440 Jones, T., Christopher, S. and Quaas, J.: A six year satellite-based assessment of the regional
441 variations in aerosol indirect effects, Atmos. Chem. Phys., 8(6), 20349–20397,
442 doi:10.5194/acpd-8-20349-2008, 2008.

443 Kahn, B. H., Schreier, M. M., Yue, Q., Fetzer, E. J., Irion, F. W., Platnick, S., Wang, C., Nasiri,

444 S. L. and L'Ecuyer, T. S.: Pixel-scale assessment and uncertainty analysis of AIRS and MODIS
445 ice cloud optical thickness and effective radius, J. Geophys. Res. Atmos., 120, 11,669–11,689,
446 doi:10.1002/2015JD024039.Received, 2015.

447 Kaufman, Y. J. and Koren, I.: Smoke and Pollution Aerosol Effect on Cloud Cover, Science (80-
448 .)., 313(August), 655–658, 2006.

449 King, M., Tsay, S., Platnick, S., Wang, M. and Liou, K.-N.: Cloud retrieval algorithms for
450 MODIS: Optical thickness, effective particle radius, and thermodynamic phase, MODIS
451 Algorithm Theor. Basis Doc. No. ATBD-MOD-05, 1997.

452 Klein, P. M., Hu, X. M., Shapiro, A. and Xue, M.: Linkages Between Boundary-Layer Structure
453 and the Development of Nocturnal Low-Level Jets in Central Oklahoma, Boundary-Layer
454 Meteorol., 158(3), 383–408, doi:10.1007/s10546-015-0097-6, 2015.

455 Koch, D. and Del Genio, a. D.: Black carbon semi-direct effects on cloud cover: Review and
456 synthesis, Atmos. Chem. Phys., 10(16), 7685–7696, doi:10.5194/acp-10-7685-2010, 2010.

457 Koren, I., Kaufman, Y. J., Remer, L. and Martins, J. V: Measurement of the effect of Amazon
458 smoke on inhibition of cloud formation., Science, 303(5662), 1342–1345,
459 doi:10.1126/science.1089424, 2004.

460 Koren, I., Martins, J. V., Remer, L. and Afargan, H.: Smoke Invigoration Versus Inhibition of
461 Clouds over the Amazon, Science (80-.)., 946(2008), doi:10.1126/science.1159185, 2009.

462 Lamsal, L. N., Duncan, B. N., Yoshida, Y., Krotkov, N. a., Pickering, K. E., Streets, D. G. and
463 Lu, Z.: U.S. NO2 trends (2005–2013): EPA Air Quality System (AQS) data versus improved
464 observations from the Ozone Monitoring Instrument (OMI), Atmos. Environ., 110(2), 130–143,
465 doi:10.1016/j.atmosenv.2015.03.055, 2015.

466 Lee, M. I., Schubert, S. D., Suarez, M. J., Schemm, J. K. E., Pan, H. L., Han, J. and Yoo, S. H.:
467 Role of convection triggers in the simulation of the diurnal cycle of precipitation over the United
468 States Great Plains in a general circulation model, J. Geophys. Res. Atmos.,
469 doi:10.1029/2007JD008984, 2008.

470 Lee, S. S. and Penner, J. E.: Aerosol effects on ice clouds: Can the traditional concept of aerosol
471 indirect effects be applied to aerosol-cloud interactions in cirrus clouds?, Atmos. Chem. Phys.,
472 10(21), 10345–10358, doi:10.5194/acp-10-10345-2010, 2010.

473 Lee, S. S., Donner, L. J. and Phillips, V. T. J.: Sensitivity of aerosol and cloud effects on
474 radiation to cloud types: comparison between deep convective clouds and warm stratiform
475 clouds over one-day period, Atmos. Chem. Phys., 9(7), 2555–2575, doi:10.5194/acp-9-2555-
476 2009, 2009.

477 Liou, K. N.: Cirrus clouds and climate, in McGraw-Hill Yearbook of Science and Technology,
478 pp. 51 – 53., 2005.

479 Maddox, R.: Large-Scale Meteorological Conditions Associated with Midlatitude, Mesoscale
480 Convective Complexes, Mon. Weather Rev., 111(7), 1475–1493, doi:10.1175/1520-
481 0493(1983)111<1475:LSMCAW>2.0.CO;2, 1983.

482 Martins, J. V., Marshak, a., Remer, L. a., Rosenfeld, D., Kaufman, Y. J., Fernandez-Borda, R.,
483 Koren, I., Correia, a. L., Zubko, V. and Artaxo, P.: Remote sensing the vertical profile of cloud
484 droplet effective radius, thermodynamic phase, and temperature, Atmos. Chem. Phys., 11(18),
485 9485–9501, doi:10.5194/acp-11-9485-2011, 2011.

Massey, F. J.: The Kolmogorov-Smirnov Test for Goodness of Fit, J. Am. Stat. Assoc., 46(253), 68–78, 1951.

Meyer, K. and Platnick, S.: Utilizing the MODIS 1.38 μm channel for cirrus cloud optical thickness retrievals: Algorithm and retrieval uncertainties, J. Geophys. Res. Atmos., 115(24), 1–13, doi:10.1029/2010JD014872, 2010.

Miller, L. H.: Table of Percentage Points of Kolmogorov Statistics, J. Am. Stat. Assoc., 51(273), 111–121, 1956.

Muhlbauer, A., Ackerman, T. P., Comstock, J. M., Diskin, G. S., Evans, S. M., Lawson, R. P. and Marchand, R. T.: Impact of large-scale dynamics on the microphysical properties of mid-latitude cirrus, J. Geophys. Res. Atmos., 119, 3976–3996, doi:10.1002/2013JD020035, 2014.

Panicker, A. S., Pandithurai, G. and Dipu, S.: Aerosol indirect effect during successive contrasting monsoon seasons over Indian subcontinent using MODIS data, Atmos. Environ., 44(15), 1937–1943, doi:10.1016/j.atmosenv.2010.02.015, 2010.

Platnick, S., King, M. D., Wind, B., Gray, M. and Hubanks, P.: An Initial Analysis of the Pixel-Level Uncertainties in Global MODIS Cloud Optical Thickness and Effective Particle Size Retrievals, in Passive Optical Remote Sensing of the Atmosphere and Clouds IV, vol. 5652, pp. 30–40., 2004.

Platnick, S., Ackerman, A. S., King, M. D., Wind, G., Menzel, P. W. and Frey, R.: Atmosphere L2 Cloud Product (06_L2), NASA MODIS Adaptive Processing System, Goddard Space Flight Center, USA., 2015.

Remer, L. a., Kaufman, Y. J., Levin, Z. and Ghan, S.: Model Assessment of the Ability of MODIS to Measure Top-of-Atmosphere Direct Radiative Forcing from Smoke Aerosols, J. Atmos. Sci., 59(3), 657–667, doi:10.1175/1520-0469(2002)059<0657:MAOTAO>2.0.CO;2, 2002.

Rosenfeld, D.: Explanation of the discrepancies among satellite observations of the aerosol indirect effects, Geophys. Res. Lett., 30(14), 1–4, doi:10.1029/2003GL017684, 2003.

Rosenfeld, D. and Lensky, I. M.: Satellite-Based Insights into Precipitation Formation Processes in Continental and Maritime Convective Clouds, Bull. Am. Meteorol. Soc., 79(11), 2457–2476, doi:10.1175/1520-0477(1998)079<2457:SBIIPF>2.0.CO;2, 1998.

Rosenfeld, D. and Woodley, W. L.: Spaceborne Inferences of Cloud Microstructure and Precipitation Processes: Synthesis, Insights, and Implications, Meteorol. Monogr., 29(51), 59–59, doi:10.1175/0065-9401(2003)029<0059:CSIOCM>2.0.CO;2, 2003.

Rosenfeld, D., Sherwood, S., Wood, R. and Donner, L.: Climate Effects of Aerosol-Cloud Interactions, Science (80-.)., 343, 379–380, doi:10.1126/science.1247490, 2014a.

Rosenfeld, D., Andreae, M. O., Asmi, A., Chin, M., Leeuw, G. De, Donovan, D. P., Kahn, R., Kinne, S., Kivekäs, N., Kulmala, M., Lau, W., Schmidt, K. S., Suni, T., Wagner, T., Wild, M. and Quaas, J.: Global observations of aerosol-cloud-precipitation-climate interactions, Rev. Geophys., 52, 750–808, doi:10.1002/2013RG000441.Received, 2014b.

Russell, A. R., Valin, L. C. and Cohen, R. C.: Trends in OMI NO2 observations over the United States: Effects of emission control technology and the economic recession, Atmos. Chem. Phys., 12(24), 12197–12209, doi:10.5194/acp-12-12197-2012, 2012.

527 Saide, P. E., Spak, S. N., Pierce, R. B., Otkin, J. a, Schaack, T. K., Heidinger, a K., Silva, a M.,
528 Kacenelenbogen, M., Redemann, J. and Carmichael, G. R.: Central American biomass burning
529 smoke can increase tornado severity in the U.S., Geophys. Res. Lett., (April 2011), 1–10,
530 doi:10.1002/2014GL062826.Received, 2015.

531 Shi, Y., Zhang, J., Reid, J. S., Holben, B., Hyer, E. J. and Curtis, C.: An analysis of the collection
532 5 MODIS over-ocean aerosol optical depth product for its implication in aerosol assimilation,
533 Atmos. Chem. Phys., 11(2), 557–565, doi:10.5194/acp-11-557-2011, 2011.

534 Small, J. D., Chuang, P. Y., Feingold, G. and Jiang, H.: Can aerosol decrease cloud lifetime?,
535 Geophys. Res. Lett., doi:10.1029/2009GL038888, 2009.

536 Stevens, B. and Feingold, G.: Untangling aerosol effects on clouds and precipitation in a
537 buffered system., Nature, doi:10.1038/nature08281, 2009.

538 Storelvmo, T., Hoose, C. and Eriksson, P.: Global modeling of mixed-phase clouds: The albedo
539 and lifetime effects of aerosols, J. Geophys. Res. Atmos., 116(5), 1–13,
540 doi:10.1029/2010JD014724, 2011.

541 Suzuki, K., Stephens, G. L., van den Heever, S. C. and Nakajima, T. Y.: Diagnosis of the Warm
542 Rain Process in Cloud-Resolving Models Using Joing CloudSat and MODIS Observations, J.
543 Atmos. Sci., 68(11), 2655–2670, doi:10.1175/JAS-D-10-05026.1, 2011.

544 Tan, B., Hu, J., Huang, D., Yang, W., Zhang, P., Shabanov, N. V., Knyazikhin, Y., Nemani, R.
545 R. and Myneni, R. B.: Assessment of the broadleaf crops leaf area index product from the Terra
546 MODIS instrument, Agric. For. Meteorol., 135(1-4), 124–134,
547 doi:10.1016/j.agrformet.2005.10.008, 2005.

548 Tao, W. K., Chen, J. P., Li, Z., Wang, C. and Zhang, C.: Impact of aerosols on convective clouds
549 and precipitation, Rev. Geophys., 50(2), doi:10.1029/2011RG000369, 2012.

550 Twomey, S.: The Influence of Pollution on the Shortwave Albedo of Clouds, J. Atmos. Sci.,
551 34(7), 1149–1152, doi:10.1175/1520-0469(1977)034<1149:TIOPOT>2.0.CO;2, 1977.

552 Weaver, S. J. and Nigam, S.: Variability of the great plains low-level jet: Large-scale circulation
553 context and hydroclimate impacts, J. Clim., doi:10.1175/2007JCLI1586.1, 2008.

554 Weaver, S. J., Baxter, S. and Kumar, A.: Climatic role of north American low-level jets on U.S.
555 regional tornado activity, J. Clim., doi:10.1175/JCLI-D-11-00568.1, 2012.

556 Xing, J., Mathur, R., Pleim, J., Hogrefe, C., Gan, C.-M., Wong, D. C., Wei, C., Gilliam, R. and
557 Pouliot, G.: Observations and modeling of air quality trends over 1990–2010 across the Northern
558 Hemisphere: China, the United States and Europe, Atmos. Chem. Phys., 15(5), 2723–2747,
559 doi:10.5194/acp-15-2723-2015, 2015.

560 Zhou, C. and Penner, J. E.: Aircraft soot indirect effect on large-scale cirrus clouds: Is the
561 indirect forcing by aircraft soot positive or negative?, J. Geophys. Res. D Atmos., 119, 11,303–
562 11,320, doi:10.1002/2013JD021272.Received, 2014.

563

564

565

566

Atmos. Chem. Phys. Discuss., doi:10.5194/acp-2016-289, 2016
Manuscript under review for journal Atmos. Chem. Phys.
Published: 18 April 2016

Atmospheric Chemistry and Physics Discussions

Figures

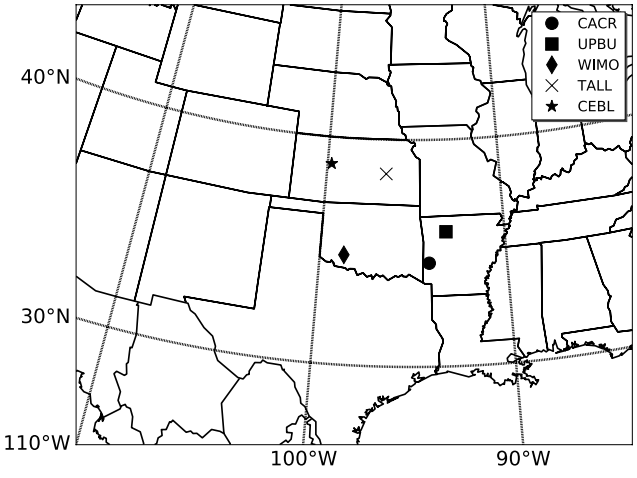

Figure 1- *Southern Great Plains (SGP) region of study with the location of five IMPROVE sites (Table 1) utilized for ground-based aerosol concentrations.*

Atmos. Chem. Phys. Discuss., doi:10.5194/acp-2016-289, 2016
Manuscript under review for journal Atmos. Chem. Phys.
Published: 18 April 2016

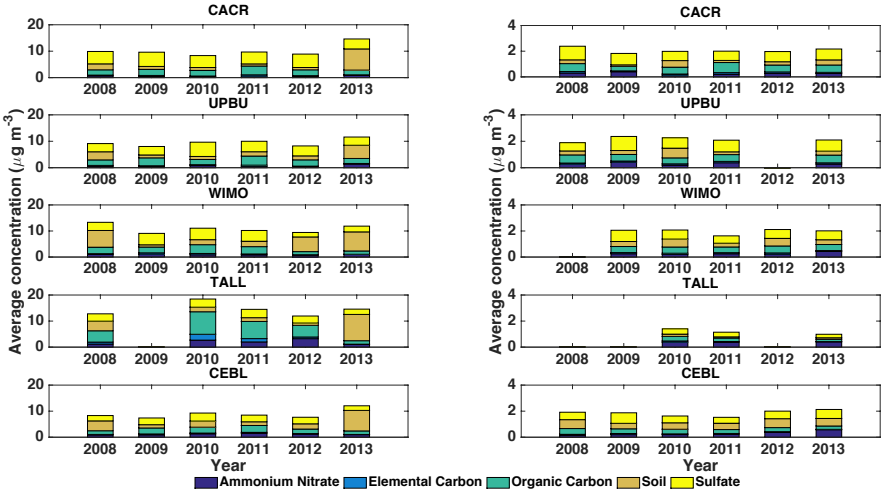

586

Figure 2- *Average aerosol mass concentration (μg m^{-3}) by composition for 2008-2013 during April-May-June (AMJ) on aerosol maximum (left column) and minimum (right column) events*

587
588
589
590
591
592
593
594
595
596
597
598
599
600
601
602
603
604
605
606
607

Atmos. Chem. Phys. Discuss., doi:10.5194/acp-2016-289, 2016
Manuscript under review for journal Atmos. Chem. Phys.
Published: 18 April 2016

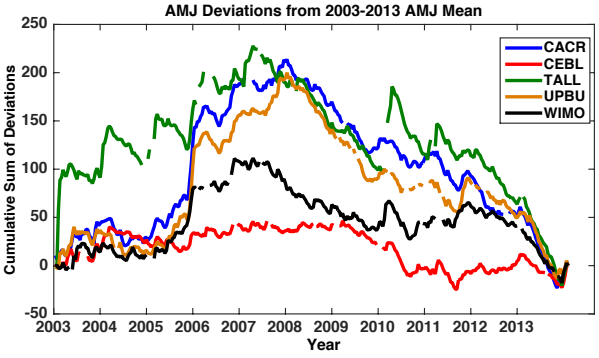

608

Figure 3- *AMJ cumulative sum of deviations from 2003-2013 AMJ mean PM2.5 concentrations. Note change point around 2008 with change in slopes from generally positive to negative (after removing the seasonality)*

609
610
611
612
613
614
615
616
617
618
619
620
621
622
623
624
625
626
627
628
629
630
631
632
633

Atmos. Chem. Phys. Discuss., doi:10.5194/acp-2016-289, 2016
Manuscript under review for journal Atmos. Chem. Phys.
Published: 18 April 2016

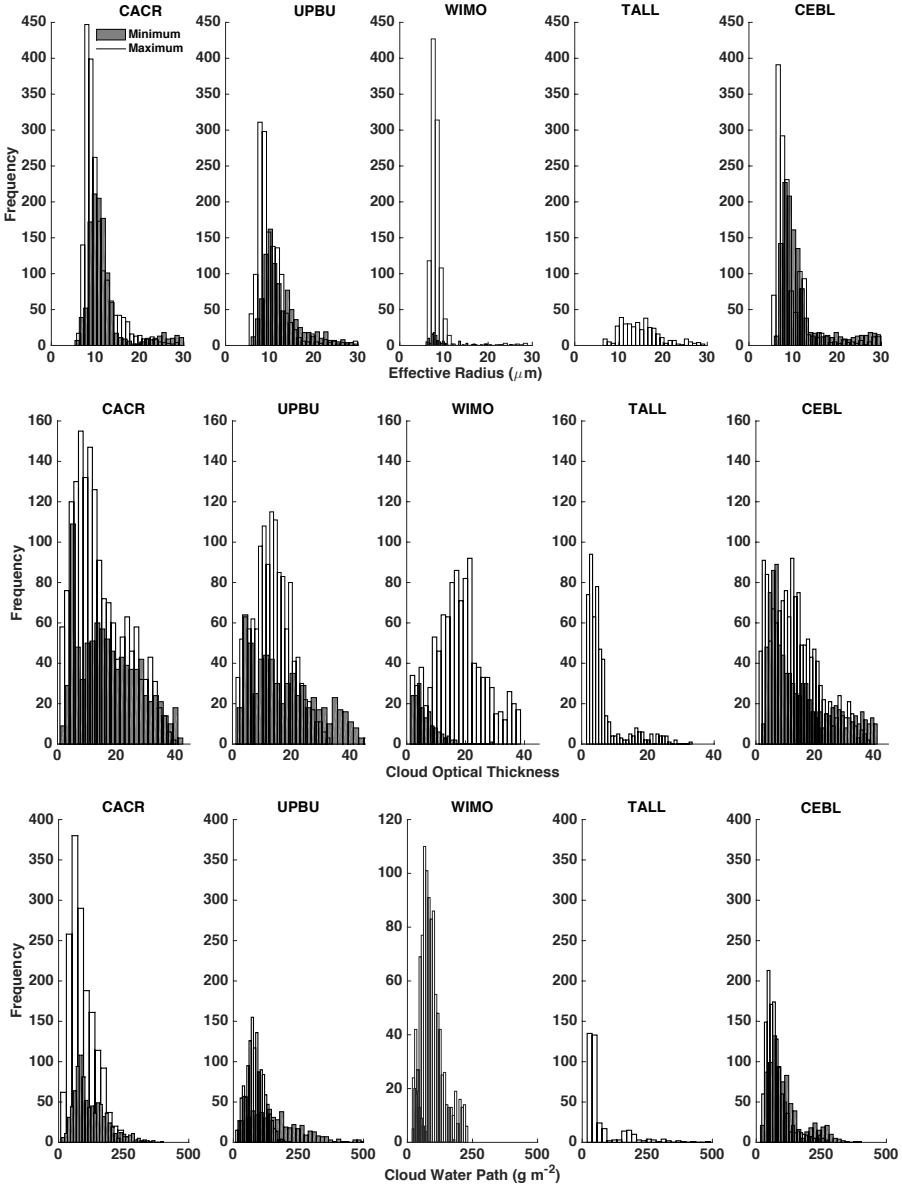

634
635
636

Figure 4- *Distributions of aerosol minimum (shaded) and maximum (outlined) liquid cloud (top row) effective radius (μm), (middle row) optical thickness and (bottom row) water path (g m^{-2}) over each site with 20% uncertainty filter applied. The satellite retrieval did not register any liquid clouds on the aerosol minimum days at TALL.*

637
638
639
640
641
642

Atmos. Chem. Phys. Discuss., doi:10.5194/acp-2016-289, 2016
Manuscript under review for journal Atmos. Chem. Phys.
Published: 18 April 2016

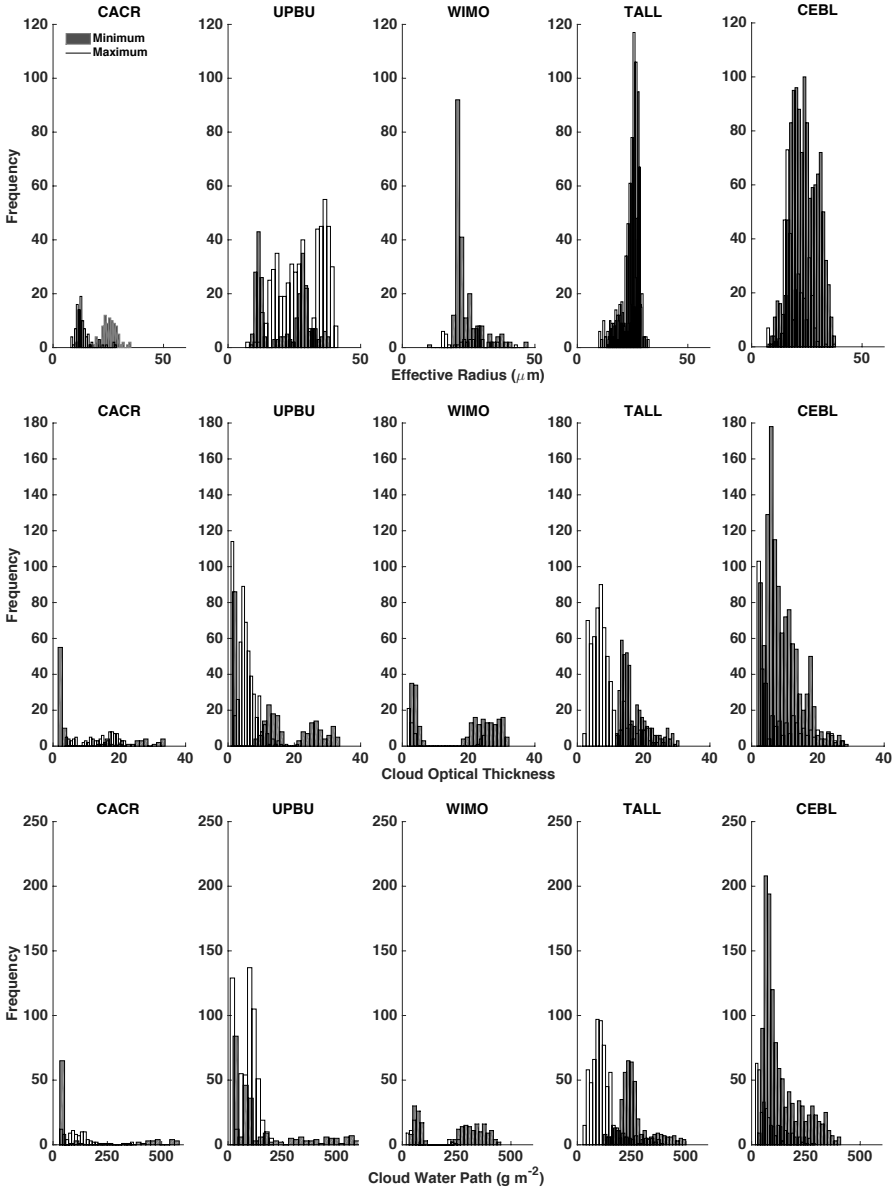

643
644
645

Figure 5- *Distributions of (top row) effective radius (μm), (middle row), cloud optical thickness and (bottom row) cloud water path (g m^{-2}) from MODIS-determined ice clouds with 20% uncertainty filter applied.*

646
647
648
649
650
651
652

Atmos. Chem. Phys. Discuss., doi:10.5194/acp-2016-289, 2016
Manuscript under review for journal Atmos. Chem. Phys.
Published: 18 April 2016

Atmospheric Chemistry and Physics Discussions

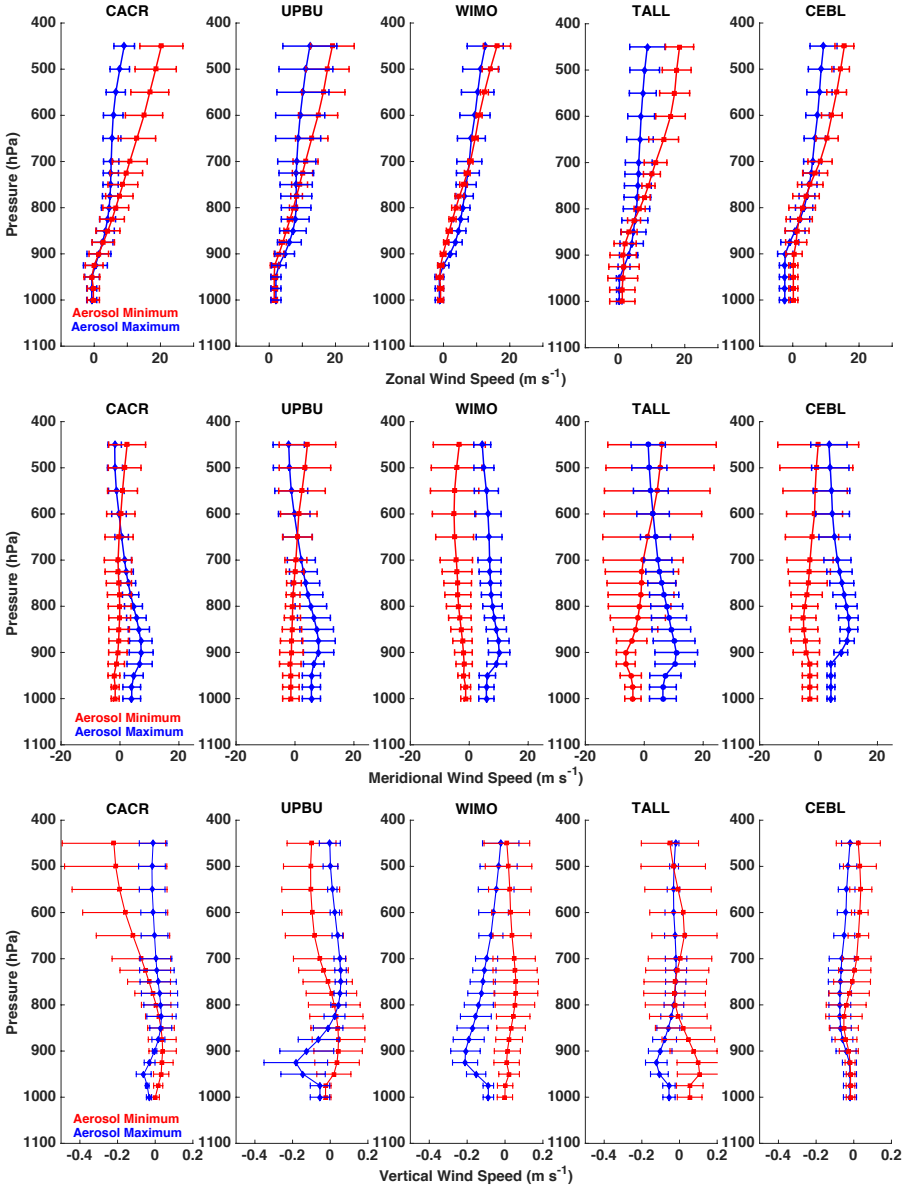

Figure 6- *North American Regional Reanalysis (NARR) daily averaged vertical wind profiles in (top row) zonal, (middle row) meridional and (bottom row) vertical wind speeds (m s^{-1}) separated by site and aerosol conditions (red = aerosol minimum; blue = aerosol maximum). Bars represent one standard deviation around average profile.*

Atmos. Chem. Phys. Discuss., doi:10.5194/acp-2016-289, 2016
Manuscript under review for journal Atmos. Chem. Phys.
Published: 18 April 2016

Atmospheric Chemistry and Physics Discussions

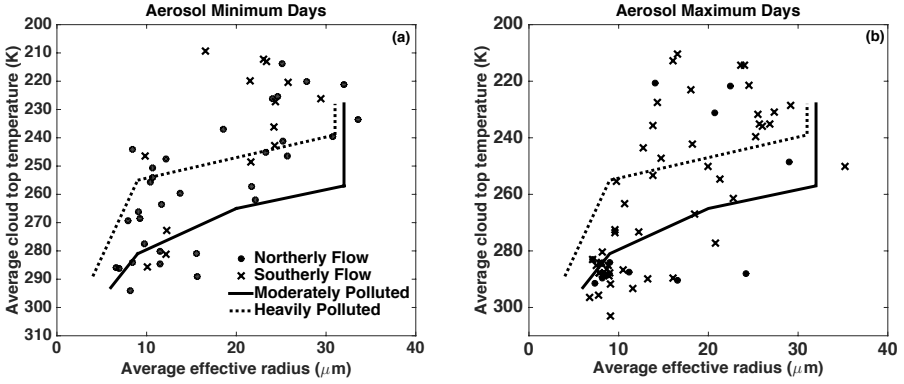

661

Figure 7- *Average cloud top temperature versus average effective radius on (a) aerosol minimum days and (b) aerosol maximum days. Markers indicate the direction of daily averaged meridional flow from NARR product as either northerly (circles) or southerly (crosses). Curves in (a,b) developed from Rosenfeld et al. (2014b) for heavy (dashed line) and moderate (solid line) pollution.*

662
663
664
665
666
667
668
669
670
671
672
673
674
675
676
677
678
679
680
681
682
683
684
685

Atmos. Chem. Phys. Discuss., doi:10.5194/acp-2016-289, 2016
Manuscript under review for journal Atmos. Chem. Phys.
Published: 18 April 2016

Atmospheric Chemistry and Physics Discussions

686 **Tables**

687

688 ***Table 1****- Summary of site geography and aerosol information*
689

Site	Latitude	Longitude	Elevation (ft)	Number of Aerosol Maximum Days 2008-2013	Number of Aerosol Minimum Days 2008-2013	AMJ Aerosol Minimum Threshold (μg m^{-3})	AMJ Aerosol Maximum Threshold (μg m^{-3})
Caney Creek (CACR)	34.4544N	-94.1429	683	27	23	4.06	11.4
Upper Buffalo Wilderness (UPBU)	35.8258N	-93.203	722	27	23	4.0	11.1
Wichita Mountains (WIMO)	34.7323N	-98.713	509	21	22	3.5	10.6
Tallgrass (TALL)	38.4341N	-96.5602	390	16	4	1.9	13.6
Cedar Bluff (CEBL)	38.7701N	-99.7634	665	26	25	2.9	8.8

690
691
692
693
694
695
696
697
698
699
700
701
702
703
704
705
706
707
708
709
710
711
712
713

Atmos. Chem. Phys. Discuss., doi:10.5194/acp-2016-289, 2016
Manuscript under review for journal Atmos. Chem. Phys.
Published: 18 April 2016

Atmospheric Chemistry and Physics Discussions

Table 2- *Statistics of liquid cloud properties over each site on both aerosol minimum and maximum days with 20% uncertainty filter applied (top) and no filter applied (bottom).*

Site	Aerosol Minimum Avg. r_{eff} (μm)	Aerosol Maximum Avg. R_E (μm)	Aerosol Minimum Avg. COT	Aerosol Maximum Avg. COT	Aerosol Minimum Avg. CWP (gm^{-2})	Aerosol Maximum Avg. CWP (gm^{-2})
CACR	17.9 (9.9)	10.9 (3.8)	12.3 (5.3)	14.8 (8.7)	123.5 (65.2)	92.8 (48.4)
UPBU	13.3 (5.3)	10.4 (3.5)	19.3 (10.8)	13.9 (6.4)	159.9 (102.1)	84.7 (34.9)
WIMO	10.5 (4.9)	8.3 (2.1)	7.5 (4.1)	18.4 (8.2)	43.8 (19.6)	93.7 (44.8)
TALL	N/A	14.9 (4.6)	N/A	7.5 (6.0)	N/A	74.9 (76)
CEBL	12.6 (6.4)	9.2 (4.6)	16.1 (10.5)	14.6 (7.8)	111.5 (70.3)	76.2 (44.3)

Site	Aerosol Minimum Avg. r_{eff} (μm)	Aerosol Maximum Avg. R_E (μm)	Aerosol Minimum Avg. COT	Aerosol Maximum Avg. COT	Aerosol Minimum Avg. CWP (gm^{-2})	Aerosol Maximum Avg. CWP (gm^{-2})
CACR	12.0 (4.8)	10.6 (3.6)	23.3 (17.3)	19.9 (15.9)	172.2 (125)	119.5 (188)
UPBU	12.7 (4.4)	10.3 (3.6)	37.9 (29.6)	14.3 (9.2)	303.7 (253.4)	90.4 (44.5)
WIMO	9.8 (5.3)	8.8 (3.4)	7.9 (12.7)	17.3 (10)	56 (81)	95.9 (52)
TALL	N/A	16.2 (5.6)	N/A	5.3 (5.2)	N/A	62.2 (68.7)
CEBL	11.9 (5.5)	10.1 (5)	25 (22.8)	12.8 (11.9)	177.2 (145)	88.7 (79.8)

Atmos. Chem. Phys. Discuss., doi:10.5194/acp-2016-289, 2016
Manuscript under review for journal Atmos. Chem. Phys.
Published: 18 April 2016

Atmospheric Chemistry and Physics Discussions

Table 3- *Statistics of ice cloud properties over each site on both aerosol minimum and maximum days with 20% uncertainty filter applied (top) and with no filter applied (bottom).*

Site	Aerosol Minimum Avg. r_{eff} (μm)	Aerosol Maximum Avg. r_{eff} (μm)	Aerosol Minimum Avg. COT	Aerosol Maximum Avg. COT	Aerosol Minimum Avg. CWP (gm^{-2})	Aerosol Maximum Avg. CWP (gm^{-2})
CACR	25.3 (2.7)	13.8 (1.3)	3.8 (4.1)	6.3 (2.7)	65 (85.5)	53.8 (24.3)
UPBU	21.3 (9)	27.9 (8.2)	13.7 (10.5)	5.2 (3)	162.2 (167.3)	86.5 (45.5)
WIMO	24.0 (5.3)	25.4 (6.6)	17.4 (10.9)	7.2 (9)	233.6 (136.2)	85.6 (81.7)
TALL	24.8 (4.1)	23.9 (4.3)	17.2 (4.4)	8.4 (4.8)	262.5 (75)	118.7 (64)
CEBL	24 (5.9)	19.4 (5)	9.2 (5.1)	8.1 (6.9)	136.4 (87.3)	83.0 (62.9)

Site	Aerosol Minimum Avg. r_{eff} (μm)	Aerosol Maximum Avg. r_{eff} (μm)	Aerosol Minimum Avg. COT	Aerosol Maximum Avg. COT	Aerosol Minimum Avg. CWP (gm^{-2})	Aerosol Maximum Avg. CWP (gm^{-2})
CACR	23.6 (2.8)	13.4 (3.8)	78.3 (27.9)	13.8 (5.4)	1145.2 (407.3)	116.8 (67.6)
UPBU	22.5 (9.4)	27.4 (8.0)	41.5 (24.5)	4.7 (4.8)	576.6 (447)	72.3 (49)
WIMO	21.8 (7.1)	19.0 (6.4)	33 (21.5)	33.6 (22.2)	420.8 (292.2)	340.4 (219.5)
TALL	25.4 (3.7)	22.9 (5.3)	24.6 (14.5)	6.23 (5.8)	393.5 (254.8)	86.2 (71.3)
CEBL	24.0 (6.5)	19.4 (6.1)	9.5 (7)	14.2 (17.5)	135 (89)	152 (183.5)

Atmos. Chem. Phys. Discuss., doi:10.5194/acp-2016-289, 2016
Manuscript under review for journal Atmos. Chem. Phys.
Published: 18 April 2016

Atmospheric Chemistry and Physics Discussions

754 ***Table 4-*** *Percent of event days with given meridional flow direction*
755

Site	Aerosol Minimum Days (Southward %: Northward %)	Aerosol Maximum Days (Southward %: Northward %)
CACR	70:30	41:59
UPBU	83:17	27:73
WIMO	77:23	9:91
TALL	100:0	19:81
CEBL	84:16	15:85

756
757
758